

A Density Functional Study of Oxygen Atom Transfer Reactions between Biological Oxygen Atom Donors and Molybdenum(IV) Bis(dithiolene) Complexes

Anders Thapper,^{*†} Robert J. Deeth,^{*‡} and Ebbe Nordlander^{*‡}

Inorganic Chemistry, Chemical Center, Lund University, Box 124, S-221 00 Lund, Sweden, and Inorganic Computational Chemistry Group, Department of Chemistry, University of Warwick, Coventry CV4 7AL, U.K.

Received June 5, 2002

Density functional calculations have been used to investigate oxygen atom transfer reactions from the biological oxygen atom donors trimethylamine *N*-oxide (Me₃NO) and dimethyl sulfoxide (DMSO) to the molybdenum(IV) complexes [MoO(mnt)₂]²⁻ and [Mo(OCH₃)(mnt)₂]⁻ (mnt = maleonitrile-1,2-dithiolate), which may serve as models for mononuclear molybdenum enzymes of the DMSO reductase family. The reaction between [MoO(mnt)₂]²⁻ and trimethylamine *N*-oxide was found to have an activation energy of 72 kJ/mol and proceed via a transition state (TS) with distorted octahedral geometry, where the Me₃NO is bound through the oxygen to the molybdenum atom and the N–O bond is considerably weakened. The computational modeling of the reactions between dimethyl sulfoxide (DMSO) and [MoO(mnt)₂]²⁻ or [Mo(OCH₃)(mnt)₂]⁻ indicated that the former is energetically unfavorable while the latter was found to be favorable. The addition of a methyl group to [MoO(mnt)₂]²⁻ to form the corresponding *des*-oxo complex not only lowers the relative energy of the products but also lowers the activation energy. In addition, the reaction with [Mo(OCH₃)(mnt)₂]⁻ proceeds via a TS with trigonal prismatic geometry instead of the distorted octahedral TS geometry modeled for the reaction between [MoO(mnt)₂]²⁻ and Me₃NO.

Introduction

The mononuclear molybdenum-containing enzymes constitute a diverse class of enzymes involved in the sulfur, carbon, and nitrogen metabolic cycles.^{1,2} They all share a common cofactor, an organic pterin containing a dithiolene moiety (molybdopterin, Figure 1).² In general, these enzymes are involved in transferring an oxygen atom to or from a biological oxygen acceptor/donor.

The dimethyl sulfoxide (DMSO) reductase family is a subgroup of the mononuclear molybdenum enzymes which, apart from DMSO reductase, also contains enzymes such as trimethylamine *N*-oxide (Me₃NO) reductase and dissimilatory nitrate reductase. There are a number of published crystal structures of enzymes from this family, most of them being of DMSO reductase from two different bacteria, *Rhodobacter*

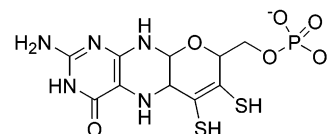


Figure 1. Schematic structure of molybdopterin. In several prokaryotic enzymes, nucleotides (AMP, GMP, IMP) are coordinated to the phosphate side chain of the pyrene (pyrene) ring.

capsulatus^{3–6} and *Rhodobacter sphaeroides*.^{7,8} In addition, the crystal structures of oxidized Me₃NO reductase from *Shewanella massilia*,⁹ dissimilatory nitrate reductase from

* To whom correspondence should be addressed. Fax: +46 46 222 4439 (E.N.). E-mail: Ebbe.Nordlander@inorg.lu.se (E.N.).

† Lund University.

‡ University of Warwick.

(1) Hille, R. *Chem. Rev.* **1996**, *96*, 2757.

(2) Collison, D.; Garner, C. D.; Joule, J. A. *Chem. Soc. Rev.* **1996**, *25*, 25.

(3) Schneider, F.; Löwe, J.; Huber, R.; Schindelin, H.; Kisker, C.; Knäblein, J. *J. Mol. Biol.* **1996**, *263*, 53.

(4) McAlpine, A. S.; McEwan, A. G.; Shaw, A. L.; Bailey, S. *J. Biol. Inorg. Chem.* **1997**, *2*, 690.

(5) McAlpine, A. S.; McEwan, A. G.; Bailey, S. *J. Mol. Biol.* **1998**, *275*, 613.

(6) Bray, R. C.; Adams, B.; Smith, A. T.; Bennett, B.; Bailey, S. *Biochemistry* **2000**, *39*, 11258.

(7) Schindelin, H.; Kisker, C.; Hilton, J.; Rajagopalan, K. V.; Rees, D. C. *Science* **1996**, *272*, 1615.

(8) Li, H.-K.; Temple, C.; Rajagopalan, K. V.; Schindelin, H. *J. Am. Chem. Soc.* **2000**, *122*, 7673.

(9) Czjzek, M.; Dos Santos, J.-P.; Pommier, J.; Giordane, G.; Méjean, V.; Haser, R. *J. Mol. Biol.* **1998**, *284*, 435.

Desulfovibrio desulfuricans,¹⁰ and formate dehydrogenase H from *Escherichia coli*¹¹ have been published. The active sites of all members of the DMSO reductase family consist of a molybdenum atom that is coordinated by two molybdopterin through their dithiolene moieties. The molybdenum atom is also coordinated to an amino acid residue—the oxygen atom of a serine residue in the case of DMSO reductase and Me₃NO reductase, and the sulfur atom of a cysteine residue in the case of nitrate reductase. In the oxidized form of DMSO reductase from *R. sphaeroides* and nitrate reductase there is one oxo ligand coordinated to molybdenum. In the corresponding reduced forms of the enzymes, the molybdenum has no oxo ligand. In contrast, in the structures of DMSO reductase from *R. capsulatus* and Me₃NO reductase there is one more oxo ligand, giving a dioxomolybdenum(VI)/monooxomolybdenum(IV) couple. This would result in an unusual seven-coordinate molybdenum(VI) site if both pterins were fully coordinated. Two recent studies of DMSO reductase from *R. sphaeroides*⁸ and *R. capsulatus*⁶ suggest that this discrepancy in the crystal structures might originate from a minor disorder in the position of the molybdenum atom in some structures that could have been interpreted as an extra oxo group. The disorder is proposed to originate from an oxidation of the active site by buffer solution(s), resulting in a five-coordinate dioxomolybdenum with one coordinated pterin, one oxygen from serine, and the other pterin at a nonbonding distance; this coordination has been observed in three of the published structures.^{3,6,8}

The reaction between a reduced molybdenum center and an oxygen-donating substrate has been proposed to proceed via a transition state where the substrate oxygen atom binds directly to the molybdenum atom.^{7,12} This proposal is supported by a study using ¹⁸O-labeled DMSO and dithionite-reduced DMSO reductase from *R. sphaeroides*.¹³ The labeled oxygen atom could be quantitatively transferred to a water-soluble phosphine, which implies a single labile oxo group in the active site. Similarly, an ¹⁸O isotope tracer experiment has shown that the oxygen atom inserted in xanthine by xanthine oxidase (a hydroxylase; vide infra) originates at the molybdenum site.¹⁴ The proposed mechanism is also in agreement with the structure of dimethyl sulfide-reduced DMSO reductase from *R. capsulatus*.⁵ In this structure, a DMSO molecule is coordinated to the molybdenum atom in the active site.

Several model systems have been investigated as mimics of the mononuclear molybdenum enzymes. Many of them possess a Mo^{VI}O₂/Mo^{IV}O couple, but some recent model systems contain two dithiolene ligands and a Mo^{VI}O(OR)/

Mo^{IV}(OR) couple (R = Si^tBuPh₂^{15,16} or Ph^{17,18}), which may serve as better models for the active sites of members of the DMSO reductase family, in particular DMSO reductase from *R. sphaeroides*. The molybdenum complex [MoO₂(mnt)₂]²⁻ (mnt = maleonitrile-1,2-dithiolate) has previously been reported to oxidize HSO₃⁻ to HSO₄⁻, thereby acting as a functional model for sulfite oxidase,^{19–21} another mononuclear molybdenum enzyme. It has been suggested that the enzymatic mechanism for sulfite oxidation proceeds via initial coordination of sulfite to the molybdenum atom through one of the substrate oxyanion moieties,²² but kinetic evidence²³ indicates that the critical step in the sulfite oxidation mechanism is the coordination of the substrate to a Mo=O group. Similarly, oxyanion attack on the metal has been suggested for the [MoO₂(mnt)₂]²⁻ + HSO₃⁻ reaction system,^{19,20} but a computational study²⁴ indicates that the reaction proceeds via an attack of the electron lone pair of the sulfur atom on one of the oxo ligands on the molybdenum. In this study, the oxo transfer reaction was found to occur with concomitant hydrogen atom transfer from hydrogen sulfite to the other oxo ligand. Upon product release, a reverse hydrogen atom transfer from the resultant hydroxo moiety back to the sulfate ion occurs.²⁴ The biological significance of this coupled electron–proton transfer mechanism is unclear as such a mechanism has, to our knowledge, not been observed for sulfite oxidase even though hydrogen sulfite is a naturally occurring substrate.²⁵

Other computational studies of phosphine oxidation by [MoO₂(Et₂dte)₂] (Et₂dte = *N,N*-diethyldithiocarbamate)²⁶ or [MoO₂(NH₃)₂(SH)₂]²⁷ have obtained similar results favoring a direct attack on one of the oxo ligands on the molybdenum. On the other hand, it has been suggested^{28,29} that substrate oxidation (hydroxylation) in xanthine oxidase proceeds via a mechanism which differs from those discussed above; this mechanism involves the formation of a transient Mo–C(substrate) bond as well as hydride transfer to form a Mo(V)–SH species. Several computational studies of models for xanthine oxidase have been reported. These studies investigate the structure of the active site in different steps

- (10) Dias, J. M.; Than, M. E.; Humm, A.; Huber, R.; Bourenkov, G. P.; Bartunik, H. D.; Bursakov, S.; Calvete, J.; Caldeira, J.; Carneiro, C.; Moura, J. J. G.; Moura, I.; Romão, M. J. *Structure* **1999**, *7*, 65.
- (11) Boyington, J. C.; Gladyshev, V. N.; Khangulov, S. V.; Stadtman, T. C.; Sun, P. D. *Science* **1997**, *275*, 1305.
- (12) Garton, S. D.; Hilton, J.; Oku, H.; Crouse, B. R.; Rajagopalan, K. V.; Johnson, M. K. *J. Am. Chem. Soc.* **1997**, *119*, 12906.
- (13) Schultz, B. E.; Hille, R.; Holm, R. H. *J. Am. Chem. Soc.* **1995**, *117*, 7, 827.
- (14) Hille, R.; Spencer, H. J. *J. Biol. Chem.* **1987**, *262*, 11914.

- (15) Donahue, J. P.; Lorber, C.; Nordlander, E.; Holm, R. H. *J. Am. Chem. Soc.* **1998**, *120*, 3259.
- (16) Donahue, J. P.; Goldsmith, C. R.; Nadiminti, U.; Holm, R. H. *J. Am. Chem. Soc.* **1998**, *120*, 12869.
- (17) Lim, B. S.; Sung, K.-M.; Holm, R. H. *J. Am. Chem. Soc.* **2000**, *122*, 7410.
- (18) Lim, B. S.; Holm, R. H. *J. Am. Chem. Soc.* **2001**, *123*, 1920.
- (19) Das, S. K.; Chaudhury, P. K.; Biswas, D.; Sarkar, S. *J. Am. Chem. Soc.* **1994**, *116*, 9061.
- (20) Chaudhury, P. K.; Das, S. K.; Sarkar, S. *Biochem. J.* **1996**, *319*, 953.
- (21) Lorber, C.; Plutino, M. R.; Elding, L. I.; Nordlander, E. *J. Chem. Soc., Dalton Trans.* **1997**, 3997.
- (22) Bray, R. C.; Gutteridge, S.; Lamy, M. T.; Wilkinson, T. *Biochem. J.* **1983**, *211*, 241.
- (23) Brody, M. S.; Hille, R. *Biochim. Biophys. Acta* **1995**, *1253*, 133.
- (24) Thapper, A.; Deeth, R. J.; Nordlander, E. *Inorg. Chem.* **1999**, *38*, 1015.
- (25) Brody, M. S.; Hille, R. *Biochemistry* **1999**, *38*, 6668.
- (26) Bray, M. R., Ph.D. Thesis, University of Warwick, Coventry, U.K., 1997.
- (27) Pietsch, M. A.; Hall, M. B. *Inorg. Chem.* **1996**, *35*, 1273.
- (28) Howes, B. D.; Bray, R. C.; Richards, R. L.; Turner, N. A.; Bennett, B.; Lowe, D. *Biochemistry* **1996**, *35*, 1432.
- (29) Lowe, D. J.; Richards, R. L.; Bray, R. C. *Biochem. Soc. Trans.* **1997**, *25*, 1995.

Molybdenum(IV) Bis(dithiolene) Complexes

of the catalytic cycle^{30–32} and possible reaction mechanisms for the oxidation of substrates (e.g. formaldehyde,^{33,34} formamide³²). Two studies^{33,34} favor the formation of a transient Mo–C bond while a third³² indicates that such bond formation is not favored.

While there have been several computational studies of reductive half-reactions of mononuclear molybdenum enzymes, theoretical studies of oxidative half-reactions involving oxygen atom transfer from a substrate to a Mo(IV) complex remain rare—examples include a computational study of the reoxidation pathway for the Mo(IV) center in xanthine oxidase³² and the very recently published investigation of a model reaction for DMSO reductase.³⁵ In order to study the intimate mechanism(s) of substrate reductions and compare the intermediates and transition states for such reactions to related reductive half-reactions, we have attempted to model the oxidative half-reactions of trimethylamine *N*-oxide reductase and DMSO reductase using density functional theory. For computational reasons, we have used mnt^{2-} as a model for the molybdopterin. Here we wish to present a computational study of the reductions of Me_3NO by $[\text{MoO}(\text{mnt})_2]^{2-}$ and of DMSO by $[\text{MoO}(\text{mnt})_2]^{2-}$ or $[\text{Mo}(\text{OCH}_3)(\text{mnt})_2]^-$.

Results and Discussion

The starting geometries for $[\text{MoO}(\text{mnt})_2]^{2-}$ (**1**), $[\text{Mo}(\text{OCH}_3)(\text{mnt})_2]^-$ (**2**), and the substrates were optimized separately. The optimized structure of the molybdenum(IV) monooxo complex was found to have a structure that is in good agreement with published crystal structures.^{16,36} In the optimized structure of $[\text{Mo}^{\text{IV}}(\text{OCH}_3)(\text{mnt})_2]^-$ (**2**), which compares well to the crystal structures of $[\text{Mo}(\text{OR})(\text{S}_2\text{C}_2\text{Me}_2)_2]^-$ ($\text{R} = \text{Ph}, i\text{-Pr}$)^{17,18} and $[\text{Mo}(\text{OSiPh}_2(t\text{-Bu}))(\text{dithiolene})_2]^-$ (dithiolene²⁻ = benzene-1,2-dithiolate, ethylene-1,2-dithiolate),¹⁵ the Mo–O distance is 1.85 Å and the methyl group lies over one of the mnt ligands (Figure 2). The same orientation was found for the recently published computational model $[\text{Mo}(\text{OCH}_3)(\text{S}_2\text{C}_2\text{Me}_2)_2]^-$.³⁵

Reduction of Me_3NO by $[\text{MoO}(\text{mnt})_2]^{2-}$. The reduction of Me_3NO by $[\text{MoO}(\text{mnt})_2]^{2-}$ was found to have a reaction energy of –63 kJ/mol. As a starting point for this reaction, the substrate was placed about 4 Å from the molybdenum complex with the oxygen pointing toward the molybdenum atom. The Mo–O(NMe₃) distance was then shortened in a number of steps, at each of which the structure was minimized, letting all degrees of freedom [except the Mo–O(NMe₃) distance] vary. When the oxygen atom of Me_3NO enters the coordination sphere of the molybdenum, the square pyramidal structure of the starting complex, with the oxo

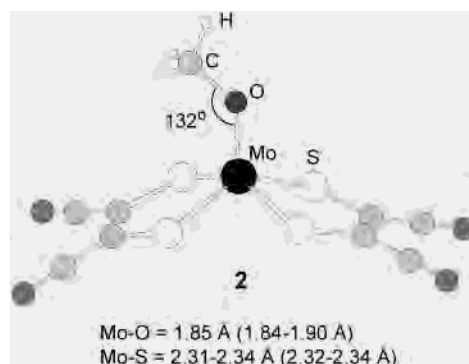


Figure 2. Modeled structure of $[\text{Mo}(\text{OCH}_3)(\text{mnt})_2]^-$ with selected distances in Å ($\epsilon = 78.8$). Numbers in parentheses are from crystal structures.^{16,18} See text for details.

ligand in the apical position, shifts into a distorted octahedral geometry. A transition state (**3**) was located for an Mo–O distance of 2.96 Å with an energy 72 kJ/mol above the starting point. In this TS, one of the sulfur atoms coordinated to the molybdenum has moved out of its position in $[\text{MoO}(\text{mnt})_2]^{2-}$ to leave an open coordination space for the entering oxygen atom; that Mo–S bond is also slightly elongated compared to the structure of $[\text{MoO}(\text{mnt})_2]^{2-}$ (2.44 Å, Figure 3). Upon further reduction of the Mo–O distance, an intermediate structure (**4**) was found with an Mo–ONMe₃ distance of 2.17 Å and an energy 65 kJ/mol above the energy at the starting point (cf. Figure 3). One of the sulfur atoms of the mnt ligands in **4** is trans to the oxo ligand with an S–Mo–O_{oxo} angle of about 160°. The trans influence of the oxo ligand makes this Mo–S bond about 0.2 Å longer than the corresponding Mo–S bond trans to the entering oxygen atom of Me_3NO , 2.61 Å vs 2.39 Å, respectively. The Me_3NO molecule coordinates with an N–O–Mo angle of 126° and an almost unperturbed bond length (1.41 Å vs 1.38 Å in free Me_3NO).

On the basis of *ab initio* studies of hydrocarbon oxidation by $[\text{MoO}_2\text{Cl}_2]$, the second “spectator” oxo ligand, which does not participate in the reaction, has been suggested to be important.³⁷ This ligand is suggested to stabilize intermediates by achieving a partial triple bond during the reaction. The spectator oxo ligand was found to play a similar role in another computational study modeling the reaction of $[\text{MoO}_2(\text{NH}_3)_2(\text{SH})_2]$ with phosphines.²⁷ The substrate attack was directed so that it allowed for a partial triple bond between the molybdenum and the spectator oxo ligand to be formed, thereby stabilizing the intermediate formed in the reaction. A partial triple bond may be stabilizing the intermediate in the reaction of $[\text{MoO}(\text{mnt})_2]^{2-}$ with Me_3NO as well, even if the effect on the reaction energy might be to stabilize the reactant compared to the product (*vide supra*).

Starting from the intermediate structure **4**, the MoO–NMe₃ distance was increased in the same way as described above. The energy of the system passed over a second maximum point. A second TS (**5**) was located at an O–N bond distance of 1.66 Å and a Mo–ONMe₃ distance of 1.92 Å (Figure 3). This TS has an energy of +71 kJ/mol relative to the starting

(30) Bray, M. R.; Deeth, R. J. *Inorg. Chem.* **1996**, *35*, 5720.

(31) Bray, M. R.; Deeth, R. J. *J. Chem. Soc., Dalton Trans.* **1997**, 4005.

(32) Ilich, P.; Hille, R. *J. Phys. Chem. B* **1999**, *103*, 5406.

(33) Bray, M. R.; Deeth, R. J. *J. Chem. Soc., Dalton Trans.* **1997**, 1267.

(34) (a) Voityuk A. A.; Albert, K.; Köstlmeier, S.; Nasluzov, V. A.; Neyman, K. M.; Hof, P.; Huber, R.; Romão, M. J.; Rösch, N. *J. Am. Chem. Soc.* **1997**, *119*, 3159. (b) Voityuk, A. A.; Albert, K.; Romão, M. J.; Huber, R.; Rösch, N. *Inorg. Chem.* **1998**, *37*, 176.

(35) Webster, C. E.; Hall, M. B. *J. Am. Chem. Soc.* **2001**, *123*, 5820.

(36) Götz, B.; Knoch, F.; Kisch, H. *Chem. Ber.* **1996**, *129*, 33.

(37) Rappé, A. K.; Goddard, W. A., III. *J. Am. Chem. Soc.* **1982**, *104*, 3287.

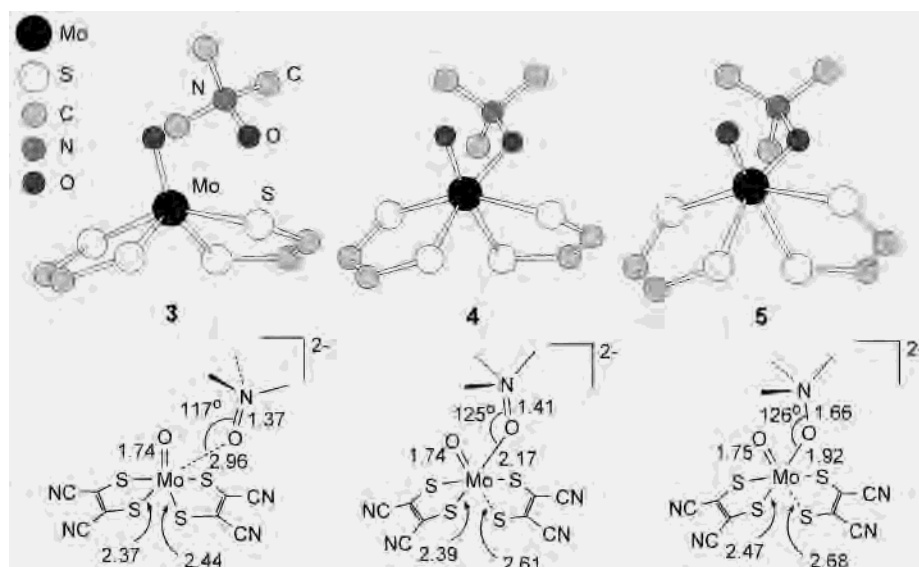


Figure 3. Calculated structure of the two transition states and the intermediate for the reaction between Me_3NO and $[\text{MoO}(\text{mnt})_2]^{2-}$ ($\epsilon = 78.8$). The hydrogens and cyanides are left out for clarity. Distances shown are in Å.

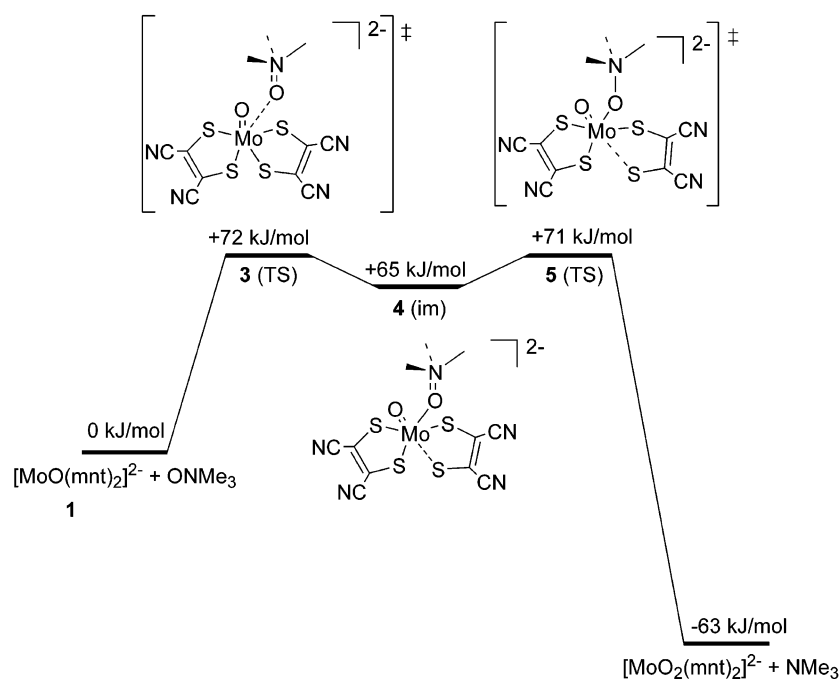


Figure 4. Energy profile for the reaction between Me_3NO and $[\text{MoO}(\text{mnt})_2]^{2-}$.

point and lies only 6 kJ/mol above the energy of the intermediate. The Mo–O and the O–N distances are both typical of single bonds. The Mo–S bonds are elongated compared to the intermediate; the Mo–S bond trans to the entering substrate is 2.47 Å, and the relatively weak bond trans to the oxo ligand is 2.68 Å. The $\text{O}_{\text{oxo}}\text{–Mo–S}$ angle is almost linear, which gives a maximal trans influence of the oxo ligand on the sulfur atom. An energy profile for the whole reaction is shown in Figure 4.

Reduction of DMSO. The complex $[\text{Mo}^{\text{IV}}\text{O}(\text{mnt})_2]^{2-}$ (**1**) may be reoxidized to $[\text{Mo}^{\text{VI}}\text{O}_2(\text{mnt})_2]^{2-}$ by Me_3NO but not by DMSO.³⁸ Our computational modeling is in agreement with this experimental observation. Thus, the reaction

between **1** and DMSO was found to have a reaction energy that is positive (+28 kJ/mol), but this value became slightly negative (–7 kJ/mol) when the reaction was modeled using $[\text{Mo}(\text{OCH}_3)(\text{mnt})_2]^-$ (**2**), in which the methoxy group mimics the serine residue in DMSO reductase. To evaluate whether there are any differences in the reactions, the reduction of DMSO by **1** or **2** was studied in the same manner as described above for the reaction of $[\text{MoO}(\text{mnt})_2]^{2-}$ and Me_3NO .

(a) Reaction with $[\text{MoO}(\text{mnt})_2]^{2-}$ (1**).** When the Mo–OS(CH_3)₂ bond in the reaction between DMSO and **1** is decreased from a starting distance of approximately 4 Å, the reaction does not proceed via a first transition state and an intermediate as in the reaction with Me_3NO (vide supra).

(38) Lorber, C. Unpublished results.

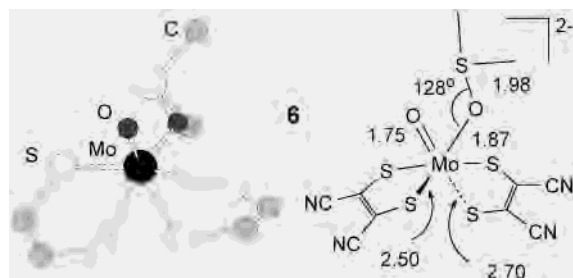


Figure 5. Calculated transition state structure for the reaction between $[\text{MoO}(\text{mnt})_2]^{2-}$ and DMSO ($\epsilon = 78.8$). The hydrogen atoms and cyanides are left out for clarity. Distances shown are in Å.

Instead, only one transition state (**6**) with a short Mo–OS–(CH₃)₂ distance, 1.87 Å, could be located. The energy of **6** is +150 kJ/mol relative to the starting point (Figure 5), reflecting the greater bond dissociation energy for the oxygen atom of DMSO compared to Me₃NO.³⁹ The bond length between the oxygen and the sulfur atom in DMSO is increased from about 1.53 Å in (DFT modeled) free DMSO to 1.98 Å in the transition state, suggesting that (partial) electron transfer has taken place at the transition state. The partial charges of the molybdenum atom and the sulfur atom at the transition state are in agreement with partial oxidation of the molybdenum atom and partial reduction of the DMSO sulfur atom.

(b) Reaction with $[\text{Mo}(\text{OCH}_3)(\text{mnt})_2]^-$ (2**).** This model reaction is closely related to the computational investigation of the reduction of DMSO by $[\text{Mo}(\text{OCH}_3)\{\text{S}_2\text{C}_2(\text{CH}_3)_2\}_2]^-$ that has recently been published by Webster and Hall.³⁵ Our results are in qualitative agreement with those obtained by Webster and Hall. The reaction between DMSO and **2** was modeled using the same approach as for the reaction with **1**, i.e., starting at a long Mo–OS(CH₃)₂ distance that was decreased in steps. Calculations were initially performed with a dielectric constant of 78.8, and it was found that the reaction proceeded via an initial transition state at +42 kJ/mol, an intermediate at +17 kJ/mol, and a second transition state at +92 kJ/mol, leading to an overall reaction energy of –7 kJ/mol for the formation of the free products. To be able to make a quantitative comparison to the results of Webster and Hall, calculations were also performed in vacuo as well as with a dielectric constant of 4 for the surrounding medium; the discussion below is an account of the modeling for $\epsilon = 4$.

The angle of attack of the DMSO molecule was optimized by a random search, and the minimum was found for an orientation in which the dimethyl sulfide moiety of the substrate approaches a perpendicular orientation with respect to the planes of the two dithiolene ligands; i.e., the attack is more “side on” than that found in the reaction with $[\text{Mo}(\text{OCH}_3)\{\text{S}_2\text{C}_2(\text{CH}_3)_2\}_2]^-$.³⁵ The energy passed over a maximum approximately 44 kJ/mol above the starting point for an Mo–OS(CH₃)₂ distance of 2.92 Å. At an Mo–OS–(CH₃)₂ distance of 2.15 Å, an intermediate structure (**7**), which lies 16 kJ/mol above the energy at the starting point, was identified. The corresponding distance in the modeled

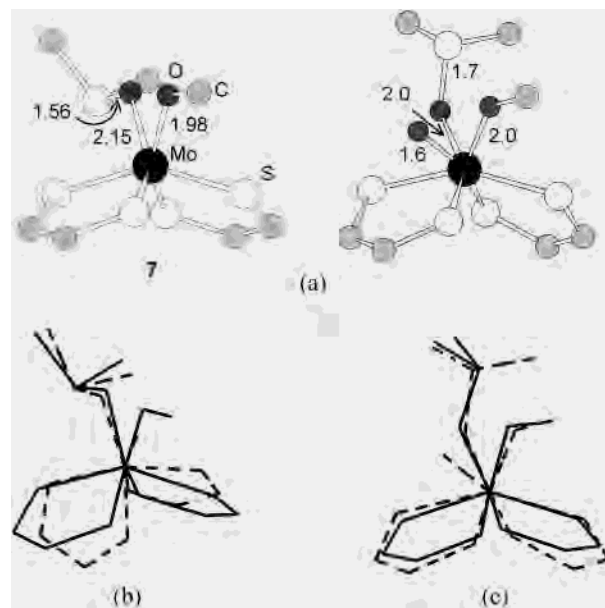


Figure 6. (a) Calculated intermediate structure for the reaction between $[\text{Mo}(\text{OCH}_3)(\text{mnt})_2]^-$ and DMSO ($\epsilon = 4$, left; cyanides and hydrogen atoms left out for clarity) and the coordination geometry of the molybdenum in the X-ray structure of DMS-reduced DMSO reductase from *R. capsulatus* (right).⁵ Distances are given in Å. The Mo–S_{dithiolene} distances are 2.33–2.38 Å in the calculated structure and 2.4–2.5 Å in the enzyme. (b) Overlay plot of the coordination geometry of Mo in the crystal structure of $[\text{Mo}^{\text{VI}}\text{O}(\text{DMSO})(3,6\text{-dbcate})_2]$ (broken line) and in the modeled “unrotated” intermediate in the reaction of $[\text{Mo}(\text{OCH}_3)(\text{mnt})_2]^-$ with DMSO (solid line). (c) Overlay plot of the coordination around Mo in DMSO reductase from *R. capsulatus* (broken line) and in the modeled “rotated” intermediate in the reaction of $[\text{Mo}(\text{OCH}_3)(\text{mnt})_2]^-$ with DMSO (solid line). See text for details.

$[\text{Mo}^{\text{VI}}(\text{OCH}_3)(\text{DMSO})\{\text{S}_2\text{C}_2\text{Me}_2\}_2]^-$ complex (Webster and Hall³⁵) is 2.27 Å. The coordination geometry around the molybdenum in **7** is a twisted trigonal prism, with a twist angle of 15°, which is markedly different from the distorted octahedral intermediate found in the reaction of Me₃NO and $[\text{MoO}(\text{mnt})_2]^{2-}$ but similar to the active site structure of DMS-reduced DMSO reductase from *R. capsulatus* (Figure 6a), apart from the additional oxo ligand found in the enzyme,⁵ which probably is a result of a disorder in the crystal structure (vide supra).⁸ In the modeled intermediate (**7**), the coordinated DMSO has an S–O distance of 1.56 Å, comparable to free DMSO and virtually identical to the distance obtained by Webster and Hall.³⁵ All Mo–S bonds are in the range 2.33–2.40 Å, and the Mo–OCH₃ bond is 1.98 Å.

As shown in Figure 6b, the orientation of the coordinated DMSO molecule in the intermediate is similar to that found in $[\text{Mo}^{\text{VI}}\text{O}(\text{DMSO})(3,6\text{-dbcate})_2]$ (3,6-dbcate = 3,6-di-*tert*-butylcatecholate),^{40,41} the crystal structure of which reveals that the Mo–OS(CH₃)₂ distance is 2.08 Å and the O–S(CH₃)₂ distance is 1.55 Å. In the structure of DMS-reduced *R. capsulatus* DMSO reductase, the O–S_{DMSO} distance is 1.7 Å and the Mo–O_{DMSO} distance 2.0 Å but the orientation of the DMSO molecule is different from the modeled reaction

(40) Thapper, A.; Lorber, C.; Fryxelius, J.; Behrens, A.; Nordlander, E. *J. Inorg. Biochem.* **2000**, *79*, 67.

(41) Liu, C.-M.; Restorp, P.; Nordlander, E.; Pierpont, C. G. *Chem. Commun.* **2001**, 2686.

(39) Donahue, J. P.; Holm, R. H. *Polyhedron* **1993**, *12*, 571.

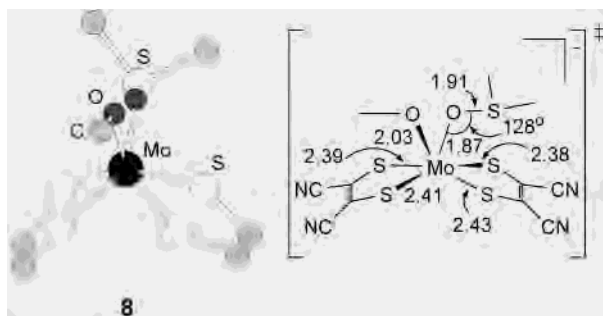


Figure 7. Calculated transition state structure for the reaction between $[\text{Mo}(\text{OCH}_3)(\text{mnt})_2]^-$ and DMSO. The hydrogen atoms and cyanides are left out for clarity. Distances shown are in Å.

intermediate. By rotation of the DMSO molecule in the model, a second structure of the complex between $[\text{Mo}(\text{OCH}_3)(\text{mnt})_2]^-$ and DMSO was minimized and found to be about 35 kJ/mol higher in energy than the “unrotated” intermediate. A comparison of the enzyme structure and the “rotated” model structure (**7a**) is shown in Figure 6c. It is possible that the surrounding protein in the enzyme stabilizes this alternative coordination of the DMSO molecule rather than the orientation that is energetically most favorable in a small inorganic molybdenum complex.

Starting from the intermediate (**7**), the $\text{O}-\text{S}(\text{CH}_3)_2$ bond length was increased and a TS (**8**) was found, the structure of which is still best described as a distorted trigonal prism (Figure 7). None of the sulfur atoms of the mnt ligands are directly trans to any oxygen atom, and the four $\text{Mo}-\text{S}$ distances remain approximately the same (2.38–2.43 Å). The torsion angle for the four dithiolene sulfurs is 126.0° , and the largest (dithiolene) $\text{S}-\text{Mo}-\text{S}$ angle is 154.5° . In **8**, the

$\text{O}-\text{S}$ bond length of 1.91 Å and an $\text{Mo}-\text{OS}(\text{CH}_3)_2$ distance of 1.87 Å are slightly longer and slightly shorter respectively than those calculated by Webster and Hall.³⁵ The energy of **8** is approximately 60 kJ/mol above the intermediate (**7**) and 76 kJ/mol above the initial reactants.

A similar reaction pathway as that described above was derived for the in vacuo reaction; the energies of the transition states and the intermediate detected in this reaction are listed in Figure 8, in which the energy profiles for the reactions with DMSO are shown. The final product of the modeled reaction, $[\text{MoO}(\text{OCH}_3)(\text{mnt})_2]^-$, has a distorted octahedral coordination environment with a clear elongation of the $\text{Mo}-\text{S}$ bond trans to the oxo ligand. In contrast, the 1.3 Å crystal structure of oxidized *R. sphaeroides* DMSO reductase reveals that the active (six-coordinate) form has a distorted trigonal prismatic structure with all $\text{Mo}-\text{S}$ distances being approximately equal.⁸

Using the transition state structure from the reaction between DMSO and $[\text{MoO}(\text{mnt})_2]^{2-}$ ($\epsilon = 78.8$) as a starting point and adding a methoxy group to the oxo ligand led to the identification of another transition state. The structure of this transition state is distorted octahedral and approximately 50 kJ/mol higher in energy than the corresponding prismatic transition state. It appears that exchanging the oxo ligand for a methoxy group on the molybdenum not only lowers the relative energy of the product compared to the reactant but also permits the reaction to proceed via a pathway with a different geometry at the transition state.

Furthermore, when a dielectric constant of 4 was maintained, but the “rotated” intermediate (**7a**) was used as a starting point, the reaction was found to proceed via a

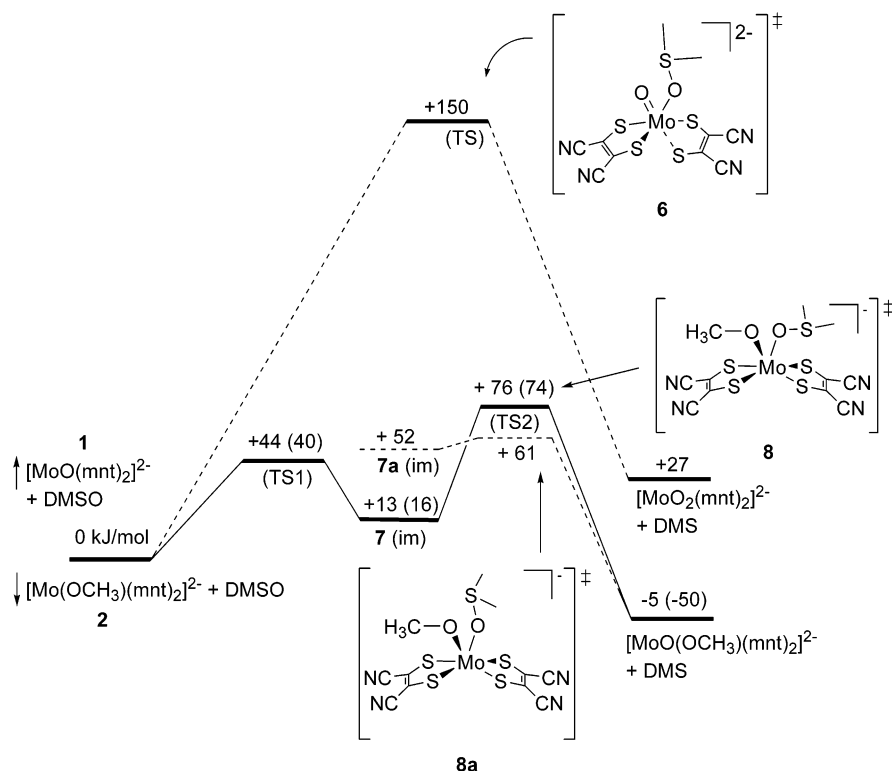


Figure 8. Energy profiles for the reactions between DMSO and $[\text{MoO}(\text{mnt})_2]^{2-}$ leading to transition state **6**: DMSO and $[\text{Mo}(\text{OCH}_3)(\text{mnt})_2]^-$ (solid line); DMSO and $[\text{Mo}(\text{OCH}_3)(\text{mnt})_2]^-$ (“rotated” intermediate, broken line). Calculated energy values for $\epsilon = 1$ are within parentheses. See text for details.

transition state (**8a**) that lies 9 kJ/mol above the intermediate which is about 15 kJ/mol lower than the energy for (**8**), while the overall reaction energy remains the same. The relative activation barrier for the conversion of the intermediate to products is thus lowered significantly when a substrate orientation that is similar to that detected in DMSO reductase is used in the computational model reaction.

A preliminary study of the reaction between nitrate and $[\text{MoO}(\text{mnt})_2]^{2-}$ was undertaken using the same methods described for the other reactions and a dielectric constant of 78.8. This reaction was found to have a positive energy of 35 kJ/mol, but when $[\text{Mo}(\text{SCH}_3)(\text{mnt})_2]^-$ (a model for the active site of nitrate reductase) was used, the total energy for the reaction became -27 kJ/mol. The reaction between the latter complex and nitrate was not modeled in detail, but it is plausible that it proceeds via a reaction pathway similar to that described above for the reaction of $[\text{Mo}(\text{OCH}_3)(\text{mnt})_2]^-$ and DMSO.

Conclusions

The reaction between $[\text{MoO}(\text{mnt})_2]^{2-}$ and Me_3NO has been demonstrated in the laboratory.³⁸ We have undertaken a density functional study of this reaction and presented a modeled reaction pathway. The reaction has an activation energy of 72 kJ/mol and proceeds via two transition states of approximately equal energy with an intermediate at 7 kJ/mol lower energy. Along the reaction pathway, an Mo–O bond is gradually forming and the N–O bond in Me_3NO gradually weakening, in keeping with the expected bridged electron-transfer mechanism. There is also a gradual change from the square pyramidal geometry of $[\text{MoO}(\text{mnt})_2]^{2-}$ to the distorted octahedral geometry of $[\text{MoO}_2(\text{mnt})_2]^{2-}$. At the second transition state, the Mo–S bond trans to the oxo ligand is elongated by approximately 0.1 Å compared to $[\text{MoO}_2(\text{mnt})_2]^{2-}$.

The similar reaction of $[\text{MoO}(\text{mnt})_2]^{2-}$ with DMSO was calculated to have a positive reaction energy and an activation energy of about 150 kJ/mol. However, when the reaction was modeled with $[\text{Mo}(\text{OCH}_3)(\text{mnt})_2]^-$, where the methoxy group mimics the serine residue found in the active site of DMSO reductase, the relative energy of the products dropped and became slightly lower than the reactants. The modeled reaction pathway, which is in qualitative agreement with that modeled by Webster and Hall (vide infra), begins such as that for the reaction of $[\text{MoO}(\text{mnt})_2]^{2-}$ with Me_3NO , but the geometries of the intermediate and the second transition state are more trigonal prismatic than octahedral. The activation energy of the reaction is significantly lowered as a consequence of this second pathway. It is possible that partial triple bonds for the *single* oxo ligands in $[\text{Mo}^{\text{IV}}\text{O}(\text{mnt})_2]^{2-}$ and $[\text{Mo}^{\text{VI}}\text{O}(\text{OCH}_3)(\text{mnt})_2]^-$ can stabilize these structures with respect to $[\text{Mo}^{\text{IV}}(\text{OCH}_3)(\text{mnt})_2]^-$ and $[\text{Mo}^{\text{VI}}\text{O}_2(\text{mnt})_2]^{2-}$, respectively, thereby favoring the oxidation of $[\text{Mo}^{\text{IV}}(\text{OCH}_3)(\text{mnt})_2]^-$ over the oxidation of $[\text{Mo}^{\text{IV}}\text{O}(\text{mnt})_2]^{2-}$. It should be noted that experimental evidence shows that $[\text{Mo}^{\text{IV}}\text{O}(\text{mnt})_2]^{2-}$ is *not* capable of reducing DMSO,³⁸ while $[\text{Mo}^{\text{IV}}(\text{OPh})(\text{S}_2\text{C}_2\text{Me}_2)_2]^-$ is capable of effecting deoxygenation of DMSO (and Me_3NO).¹⁷

In the active site of members of the DMSO reductase family of mononuclear molybdenum enzymes there is often an amino acid residue coordinated to the molybdenum, e.g. serine or cysteine. This study indicates that this amino acid residue may play a key role in stabilizing the oxidized form of the enzyme as compared to the reduced enzyme. Furthermore, the coordinated amino acid residue might facilitate a reaction mechanism involving less rearrangement of the active site structure during catalysis. Two other computational studies have investigated the importance of the cysteine residue coordinated to the molybdenum in the active site of sulfite oxidase. They suggest that the cysteine residue may modulate the redox-active d-orbital on the molybdenum atom; this would affect the redox potential and reactivity of the active site.^{42,43} It is possible that the different amino acid residues (serine, cysteine, and selenocysteine) found in the active site of members of the DMSO reductase family of molybdoenzymes play a similar role in affecting the specificity of the enzyme.

Calculations on DMSO reduction by $[\text{Mo}^{\text{IV}}(\text{OCH}_3)(\text{S}_2\text{C}_2\text{Me}_2)_2]^-$,³⁵ using geometries for the starting complex $[\text{Mo}^{\text{IV}}(\text{OCH}_3)(\text{DMSO})(\text{S}_2\text{C}_2\text{Me}_2)_2]^-$ and the product, $[\text{Mo}^{\text{VI}}(\text{OCH}_3)(\text{DMSO})(\text{S}_2\text{C}_2\text{Me}_2)_2]^-$, which are similar to those observed for reduced and oxidized forms of DMSO reductase as well as the calculated transition state (vide supra), show that the ground states of the starting complex and the product are raised with respect to the corresponding unrestrained models. Webster and Hall³⁵ point out that this is in agreement with the entatic principle.⁴⁴ Although we have not performed calculations that directly corroborate these conclusions, we note that the orientation of bound DMSO in the enzyme (vide supra) may be due to the influence of the protein and that our calculations on a model with a similar orientation of the bound substrate give results that are in qualitative as well as quantitative agreement with those of Webster and Hall. The transition state found by Webster and Hall has a structure which is closer to a regular trigonal prism than in our calculations. The relatively minor differences in structure and energies of these transition states may be due to the different dithiolene ligands used in the models and the different orientations of the substrate (DMSO).

In this study, a relatively crude model for the molybdopterin ligand, viz. mnt^{2-} , has been used. Our results do not support any involvement of the dithiolenes in any redox activity, as was suggested in the report of the first crystal structure of DMSO reductase.⁷ However, the relative simplicity of our model ligand does not permit an analysis of the possible involvement of the inherent potential redox activity of the pterin ligand itself in the enzyme mechanisms;⁴⁵ a more advanced model ligand must be used for such a study.

(42) Izumi, Y.; Glaser, T.; Rose, K.; McMaster, J.; Basu, P.; Enemark, J. H.; Hedman, B.; Hodgson, K. O.; Solomon, E. I. *J. Am. Chem. Soc.* **1999**, *121*, 10035.

(43) McNaughton, R. L.; Tipton, A. A.; Rubie, N. D.; Conry, R. R.; Kirk, M. L. *Inorg. Chem.* **2000**, *39*, 5697.

(44) (a) Vallee, B. L.; Williams, R. J. P. *Proc. Natl. Acad. Sci. U.S.A.* **1968**, *59*, 498. (b) Williams, R. J. P. *Eur. J. Biochem.* **1995**, *234*, 363.

(45) Bradshaw, B.; Collison, D.; Garner, C. D.; Joule, J. A. *Chem. Commun.* **2001**, 123.

Computational Details

The density functional calculations were performed with the Amsterdam Density Functional (ADF) program, version 2000.01,^{46–49} using an uncontracted triple- ζ STO basis set with frozen cores and an added polarization function and were carried out on the LUNARC parallel computer cluster. The implementation of the local density approximation (LDA) uses the standard Slater exchange term⁵⁰ and the correlation term due to Vosko, Wilk, and Nusair.⁵¹ Geometries were optimized at the LDA level using analytical energy gradients^{49,52} within a spin-restricted formalism. Total binding energies were calculated at the LDA geometries using Becke's 1988⁵³ and Perdew's 1986⁵⁴ gradient-corrected functionals for exchange and correlation, respectively. Transition state structures were located using the transition state algorithm of the ADF program package^{49,55} and had a single negative eigenvalue in the

Hessian matrix. For some of the calculations a COSMO type solvent correction^{56–58} was applied by assuming a solvent dielectric constant of 78.8 or 4 (see text for details). Default convergence criteria were employed throughout.

Acknowledgment. This research has been sponsored by grants from the Swedish Research Council (VR, to E.N.) and the Engineering and Physical Sciences Research Council (EPSRC, to R.J.D.). We thank the board of the LUNARC computing center (Lund University, Lund, Sweden) for access to their SGI Origin 2000 parallel computer cluster.

Supporting Information Available: Tables containing structural parameters and total energies for relevant transition states and intermediates as well as atomic coordinates for the structures depicted in Figures 2–7. This material is available free of charge via the Internet at <http://pubs.acs.org>.

IC020385H

(46) Baerends, E. J.; Ellis, D. E.; Ros., P. *Chem. Phys.* **1973**, *2*, 41.

(47) te Velde, G.; Baerends, E. J. *J. Comput. Phys.* **1992**, *99*, 84.

(48) Fonseca Guerra, C.; Snijders, J. G.; te Velde, G.; J. B. E. *Theor. Chem. Acc.* **1998**, *99*, 391.

(49) Versluis, L.; Ziegler, T. *J. Chem. Phys.* **1988**, *88*, 322.

(50) Slater, J. C. *Adv. Quantum Chem.* **1972**, *6*, 1.

(51) Vosko, S. H.; Wilk, L.; Nusair, M. *Can. J. Phys.* **1980**, *58*, 1200.

(52) Fan, L. Y.; Ziegler, T. *J. Chem. Phys.* **1991**, *95*, 7401.

(53) Becke, A. D. *Phys. Rev. A* **1988**, *38*, 3098.

(54) Perdew, J. P. *Phys. Rev. B: Condens. Matter* **1986**, *33*, 8822.

(55) Fan, L.; Ziegler, T. *J. Am. Chem. Soc.* **1992**, *114*, 10890.

(56) Klamt, A.; Schüürmann, G. *J. Chem. Soc., Perkin Trans. 2* **1993**, 799.

(57) Klamt, A. *J. Phys. Chem.* **1995**, *99*, 2224.

(58) Klamt, A.; Jones, V. *J. Chem. Phys.* **1996**, *105*, 9972.